Induction Motor controls and Implementation using dSPACE

A. ABBOU, T. NASSER, H. MAHMOUDI, M. AKHERRAZ, A. ESSADKI
Department of Electrical Engineering,
Mohamed V University, Ecole Mohamedia d'Ingenieur
BP. 765 Agdal Rabat
MOROCCO
abbou@emi.ac.ma, mahmoudi@emi.ac.ma, akherraz@emi.ac.ma, ahmed.essadki1@gmail.com

Abstract: - This paper is devoted to the modeling and dSPACE implementation of three-phase squirrel-cage induction motor control using the constant Volts per Hertz principle and rotor flux oriented control (RFOC) strategy. A fuzzy PI controller is used in the speed control loop. Experimental results are compared for two different controls using a dSPACE system with DS1104 controller board based on digital processor Texas Instruments TMS320F240 DSP.

Key-Words: - Induction Motor (IM), dSPACE, constant V/f principle, RFOC strategy , PI fuzzy.

1 Introduction

The induction motor is one of the most widely used machines in industrial applications due to its high reliability, relatively low cost, and modest maintenance requirements. With the development of power electronics technology, low cost digital Signal processing (DSP) micro-controllers and estimation techniques the induction motor an attractive component for the future high performance drives [1],[2]. The induction motor is known as a complex nonlinear system in which time-varying parameters entail an additional difficulty for developing control strategies. Based on the fact that the model can be significantly simplified if one applies the d-q Park transformation and field oriented technique also called vector control, different structures of the model exist in the literature [3],[4]. The choice of a model structure depends on the reference frame, the selected state variables and the problem at hand. Industrial applications involving induction motors are subject to control and monitoring problems.

However, induction motors can only run at their rated speed when they are connected to the main power supply. This is the reason why variable frequency drives are needed to vary the rotor speed of an induction motor. The most popular algorithm for the control of a three-phase induction motor is the V/f control approach using a natural pulse-width modulation (PWM) technique to drive a voltage-source inverter (VSI). But the performance electric drives require decoupled torque and flux control. This control is commonly provided through Field Oriented Control (FOC), which is based on decoupling of the torque-producing current component and the flux- producing component. FOC drive scheme requires current controllers and coordinate transformations [5].

The present study aims to compare experimental results for two different controls: constant V/f principle using the model of the induction motor in steady-state and indirect rotor flux oriented control (IRFOC) strategy supplied by hysteresis current-controlled inverter. The speed control loop, proposed in this paper, is provided by a PI controller based on fuzzy logic.

This paper is organized as follows: first the dynamic model of induction motor is presented, the constant V/f principle and IRFOC strategies are developed in the third section, the speed PI Fuzzy controller design is performed in the fourth section, section five present an experimental setup and results, a conclusion and reference list end the paper.

2 Induction motor model

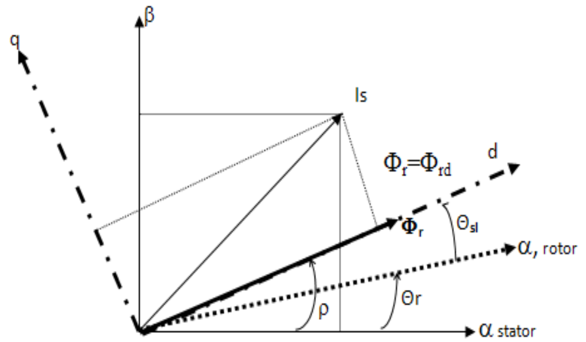

Fig.1. d-q and α-β frames

In the (d, q) oriented axes (Fig.1), the induction motor is described by the following model [6]:

$$\begin{cases} \dot{x} = f(x) + g(x)u(t) \\ y(t) = h(t) \end{cases} \qquad (1)$$

Where $x = [i_{sd} \quad i_{sq} \quad \Phi_{rd} \quad \Omega]^t$ and $u = [V_{sd} \quad V_{sq}]^t$ are respectively the state vector and the control vector.

With:

$$f(x) = \begin{bmatrix} f_1(x) \\ f_2(x) \\ f_3(x) \\ f_4(x) \end{bmatrix} = \begin{bmatrix} -\gamma.i_{sd} + k.\mu.\Phi_{rd} + p\Omega.i_{sq} + M.k.\dfrac{i_{sq}^2}{\Phi_{rd}} \\ -\gamma.i_{sq} - \mu.\Omega.\Phi_{rd} - p\Omega.i_{sd} - M.k.\dfrac{i_{sq}.i_{sd}}{\Phi_{rd}} \\ -k.\Phi_{rd} + M.k.i_{sd} \\ \eta.\Phi_{rd}.i_{sq} - \dfrac{C_r}{J} \end{bmatrix} \qquad (2)$$

$$h = [\Omega \quad \Phi_{rd}]^t \qquad (3)$$

$$g = \begin{bmatrix} \delta & 0 & 0 & 0 \\ 0 & \delta & 0 & 0 \end{bmatrix} \qquad (4)$$

And $\gamma = (R_s + (\dfrac{M}{L_r})^2.R_r).\delta = R_{sr}.\delta$, (5)

$$k = \frac{R_r}{L_r}, \qquad \mu = \frac{M}{\sigma L_s L_r} \quad \eta = \frac{pM}{JL_r},$$
$$\delta = \frac{1}{\sigma L_s}, \qquad a = \frac{M}{L_r}, \qquad \sigma = 1 - \frac{M^2}{L_s L_r}, \qquad (6)$$

The electromagnetic torque can be expressed as (Φ_{rq}=0):

$$C_e = p\frac{M}{L_r}(\Phi_{rd}.i_{sq} - \Phi_{rq}.i_{sd}) = p\frac{M}{L_r}\Phi_{rd}.i_{sq} \qquad (7)$$

3 Two control scheme for induction motor

3.1 Constant V/f principle

An improvement of open loop constant V/f principle is close loop speed control by slip regulation as shown in Figure 2. Here, the speed loop error generates the slip command ω_{sl} through a fuzzy proportional-integral (P-I) controller and limiter. The slip is added to the feedback speed signal to generate the frequency command as shown.

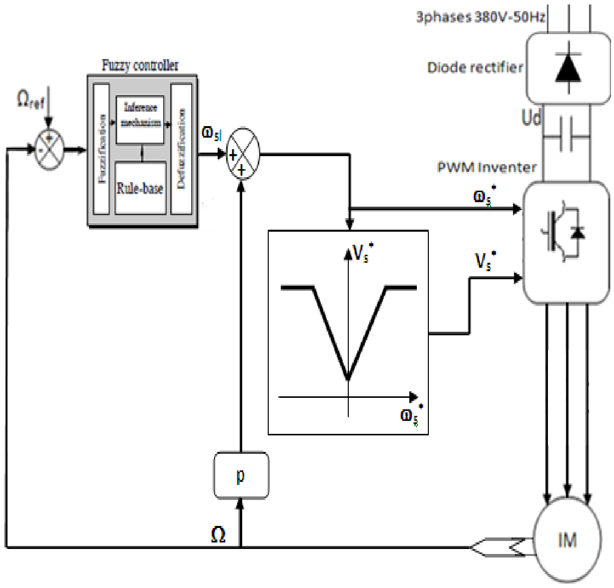

Fig. 2. Block diagram of constant V/f principle

The frequency command ω_s* also generates the voltage command through a V/f function generator, which incorporates the low-frequency stator drop compensation. Since the slip is proportional to the developed torque at constant flux (10), the scheme can be considered as an open loop torque control within a speed control loop. The feedback current signal is not used anywhere in the loop. With a step-up speed command, the machine accelerates freely with a slip limit that corresponds to the stator current or torque limit, and then settle down to the slip value at steady state as dictated y the load torque. If the command speed Ω_{ref} is reduced by a step, the drive goes into regenerative or dynamic braking mode and decelerates with constant negative slip -ω_{sl}*, as indicated in the figure.

If stator resistance R_s is neglected, electromagnetic torque can be expressed as [7]:

$$Ce = 3\frac{p}{2}(\frac{V_s}{\omega_s})^2 \frac{\omega_{sl} R_r}{R_r^2 + \omega_{sl}^2 l_r^2} \qquad (8)$$

With, ($\omega_{sl} l_r$) is the leakage reactance referred to the stator

Also, the air gap flux can be given by:

$$\Phi_m = \omega_s V_s \qquad (9)$$

In a low-slip region, (8) can be approximated as

$$Ce = 3\frac{p}{2}(\Phi_m)^2\frac{\omega_{sl}}{R_r} \qquad (10)$$

Where $R_r^2 >> \omega_{sl}^2 l_r^2$. Equation (10) is very important. It indicates that at constant flux Φ_m, the torque Ce is proportional to ω_{sl}, or at constant ω_{sl}, Ce is proportional to Φ_m^2.

The different operating regions of torque-speed curves for a variable-speed drive system with a variable-frequency, variable-voltage supply are shown in Figure 3. The inverter maximum, but short-time or transient torque capability, is limited by the peak inverter current and is somewhat lower than the machine torque capability (Figure 3). The margin permits machine breakdown torque variation by a variation of machine parameters.

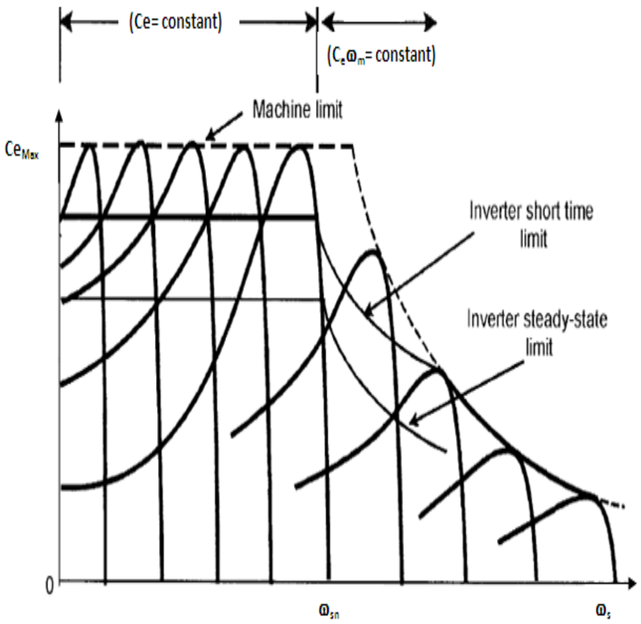

Fig.3.Torque-speed curves at variable voltage and variable frequency up to field-weakening region

3.2 RFOC Strategy

The behavior of the induction machine subjected to rotor-flux-oriented control shown in Figure 4 is similar to that of the separately excited DC machine. The space angle of the rotor flux space phasor (ρ) is obtained as the sum of the rotor angle (θ_r) and the reference value of the slip angle (θ_{sl}).

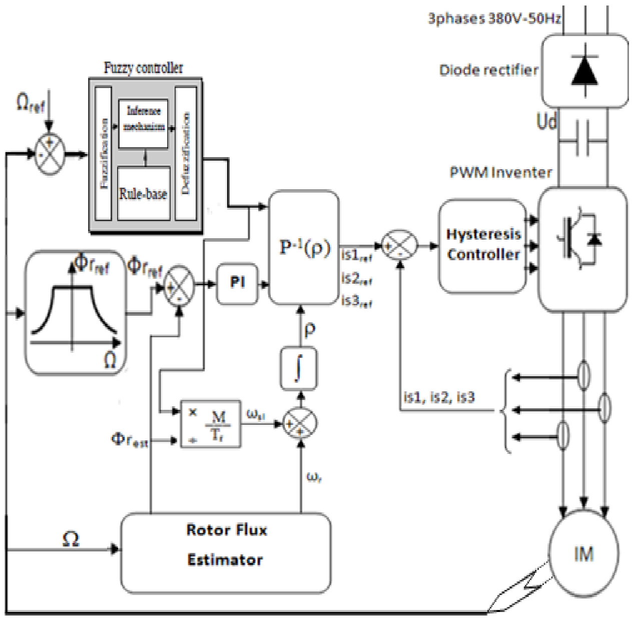

Fig.4.Block diagram of RFOC strategy

These angles are shown in Figure 1 and the stator voltage angular frequency (ω_s) is determined by the controller [7] according to which the speed of the rotor flux space phasor is

$$\omega_s = \omega_r + \omega_{sl} \qquad (11)$$

Where ω_r is the rotor electrical speed,

$$\omega_r = \frac{d\theta_r}{dt} \qquad (12)$$

And ω_{sl} is the reference value of the slip frequency,

$$\omega_{sl} = \frac{M.i_{sq}}{T_r.\Phi_{rd}} \qquad (13)$$

Furthermore,

$$\omega_s = \frac{d\rho}{dt}, \qquad (14)$$

Thus the rotor flux angle is given by

$$\rho = \theta_r + \int\frac{M.i_{sq}}{T_r.\Phi_{rd}}dt \qquad (15)$$

Note that the rotor pole position is not absolute, but is slipping with respect to the rotor at frequency ω_{sl}. The phasor diagram suggests that for decoupling control, the stator flux component of current $i_{s\alpha}$ should be aligned and the *d* axis, and the torque component of current $i_{s\beta}$ should be on the *q* axis, as shown.

In order to transform the two rotating input quantities into two stationary output quantities, we need to perform the inverse Park transformations

P(ρ). It utilizes the positional angle of the rotor flux (ρ) to do this:

$$\begin{bmatrix} i_{s\alpha} \\ i_{s\beta} \end{bmatrix} = \begin{bmatrix} \cos\rho & -\sin\rho \\ \sin\rho & \cos\rho \end{bmatrix} . \begin{bmatrix} i_{sd} \\ i_{sq} \end{bmatrix} \qquad (16)$$

3.3 Rotor flux estimation

The rotor flux components can be synthesized more easily with the help of speed and current signals. The rotor circuit equations of (α, β) equivalent circuits [8] can be given as.

$$\begin{cases} \dfrac{d\Phi_{r\alpha}}{dt} + p\Omega.\Phi_{r\beta} + R_r.i_{r\alpha} = 0 \\ \dfrac{d\Phi_{r\beta}}{dt} - p\Omega.\Phi_{r\alpha} + R_r.i_{r\beta} = 0 \end{cases} \qquad (17)$$

Adding terms $M.k.i_{s\alpha}$ and $M.k.i_{s\beta}$, respectively, on both sides of the above equations, we get

$$\begin{cases} M.k.i_{s\alpha} = \dfrac{d\Phi_{r\alpha}}{dt} + k(M.i_{s\alpha} + L_r.i_{r\alpha}) + p\Omega.\Phi_{r\beta} \\ M.k.i_{s\beta} = \dfrac{d\Phi_{r\beta}}{dt} + k(M.i_{s\beta} + L_r.i_{r\beta}) - p\Omega.\Phi_{r\alpha} \end{cases} \qquad (18)$$

Substituting equations (19) and (20), respectively, and simplifying, we get:

$$\Phi_{r\alpha} = M.i_{s\alpha} + L_r.i_{r\alpha} \qquad (19)$$

$$\Phi_{r\beta} = M.i_{s\beta} + L_r.i_{r\beta} \qquad (20)$$

$$\begin{cases} \dfrac{d\Phi_{r\alpha}}{dt} = k.M.i_{s\alpha} - p\Omega.\Phi_{r\beta} - k.\Phi_{r\alpha} \\ \dfrac{d\Phi_{r\beta}}{dt} = k.M.i_{s\beta} + p\Omega.\Phi_{r\alpha} - k.\Phi_{r\beta} \end{cases} \qquad (21)$$

Equation (21) gives rotor fluxes as functions of stator currents and speed. Therefore, knowing these signals, the fluxes and corresponding unit vector signals can be estimated. Finally,

$$\Phi_r = \sqrt{(\Phi_{r\alpha}^2 + \Phi_{r\beta}^2)} \qquad (22)$$

4 PI Fuzzy controller

The block diagram of the PI Fuzzy controller is shown in Figure 5, where the variables K_p, K_i and B are used to tune the controller.

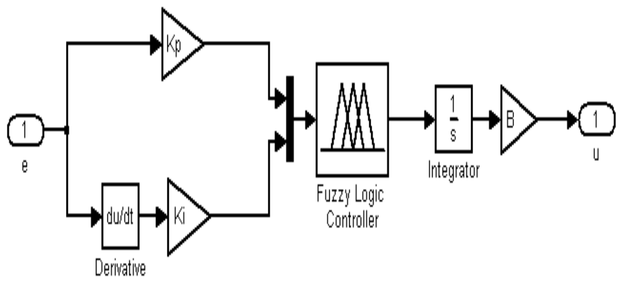

Fig.5. PI Fuzzy controller

One possible initial rule base, that can be used in drive systems for a fuzzy logic controller, consist of 49 linguistic rules, as shown in Table 1, and gives the change of the output of fuzzy logic controller in terms of two inputs:

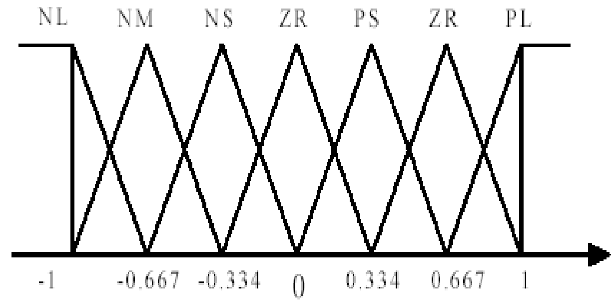

Fig. 6. Membership functions

The error (**e**) and change of error (**de**). The membership functions of these variables are given in Figure 6.

E/dE	NL	NM	NS	ZR	PS	PM	PL
PL	ZR	PS	PM	PL	PL	PL	PL
PM	NS	ZR	PS	PM	PL	PL	PL
PS	NM	NS	ZR	PS	PM	PL	PL
ZR	NL	NM	NS	ZR	PS	PM	PL
NS	NL	NL	NM	NS	ZR	PS	PM
NM	NL	NL	NL	NM	NS	ZR	PS
NL	NL	NL	NL	NL	NM	NS	ZR

Table 1: Fuzzy rules bases

In Table 1, the following fuzzy sets are used: NL negative large, NM negative medium, NS negative small, ZR zero, PS positive small, PM positive medium and PL positive large. For example, it follows from Table 2 that the first rule is:

IF **e** is NL and **de** is NL then **du** is NL (23)

The linguistic rules are in the form of IF-THEN rules and take form: IF (e is X and de is Y) then (du is Z), where X, Y, Z are fuzzy subsets for the universe of discourse of the error, change of error and change of the output. For example, X can denote the subset NEGATIVE LARGE of the error etc. On every of these universes is placed seven triangular membership functions (Figure 6). It was chosen to set these universes to normalized type for all of inputs and output. The range of universe is set to -1 to 1.

5 Experimental Setup and Results

The control algorithm has been implemented using a dSPACE board with TMS320F240 DSP. The dSPACE works on Matlab/Simulink platform which is a common engineering software and easy to understand. Another feature of the dSPACE is the Control desk which allows the graphical user interface, through the control desk the user can observe the response of the system also he can give command to the system through this interface. Real time interface is needed for the dSPACE to work. Real-time Interface (RTI) is the link between dSPACE's real-time systems and the development software MATLAB/Simulink from the Math Works. It extends Real-Time Workshop (C-code generation) for the seamless and automatic implementation of our Simulink Models on the dSPACE Real-time Hardware. This allows us to concentrate fully on the actual design process and to carry out fast design iterations. To specify a dSPACE I/O board, we can simply pick up the corresponding I/O module graphically from the RTI block library and then attach and parameterize it within Simulink.

Power circuit for the drive consist a Semikron IGBT based voltage source inverter with opto-isolation and gate driver circuit SKHI22A. The dc voltage for the VSI is achieved through a three-phase diode bridge rectifier module. A capacitive filter is used at the dc link of this module to reduce the voltage ripples.

The motor used in this experimental investigation is a three phases, 3KW, 4 poles squirrel cage induction machine, 7.2A/12.5A, 220V/380V, 50HZ and 1400rpm.

The induction motor is driven by constant V/f principle then an IRFOC algorithm included in a speed control closed-loop and run under different loads with the help of DC generator mechanically coupled to the motor and having the following characteristics: 3KW, 120V, 25A and 1500rpm.

All current and voltage are measured using LEM sensors (LEM HX15-P, LEM LV25-P), and both of them are then transformed to be a voltage ranging from 0 to ±10 volts which will be the input of A/D respectively. Figure 7 gives the experimental platform scheme used:

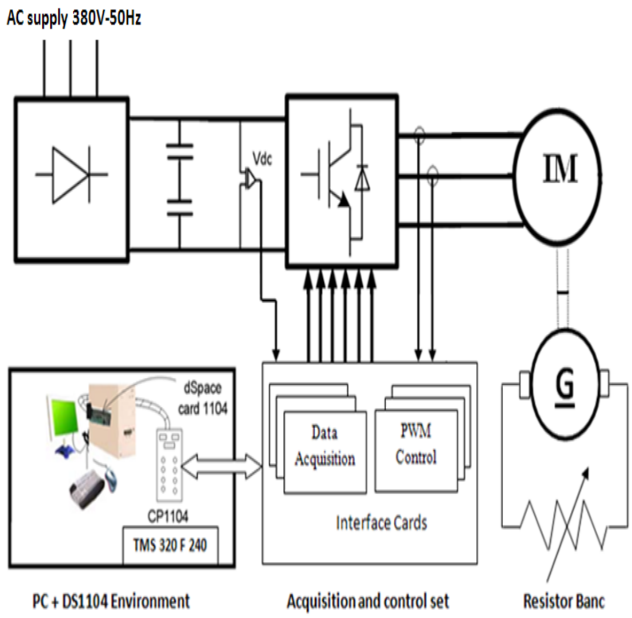

Fig. 7. Experimental test setup.

5.1 Experimental results for Constant V/f principle:

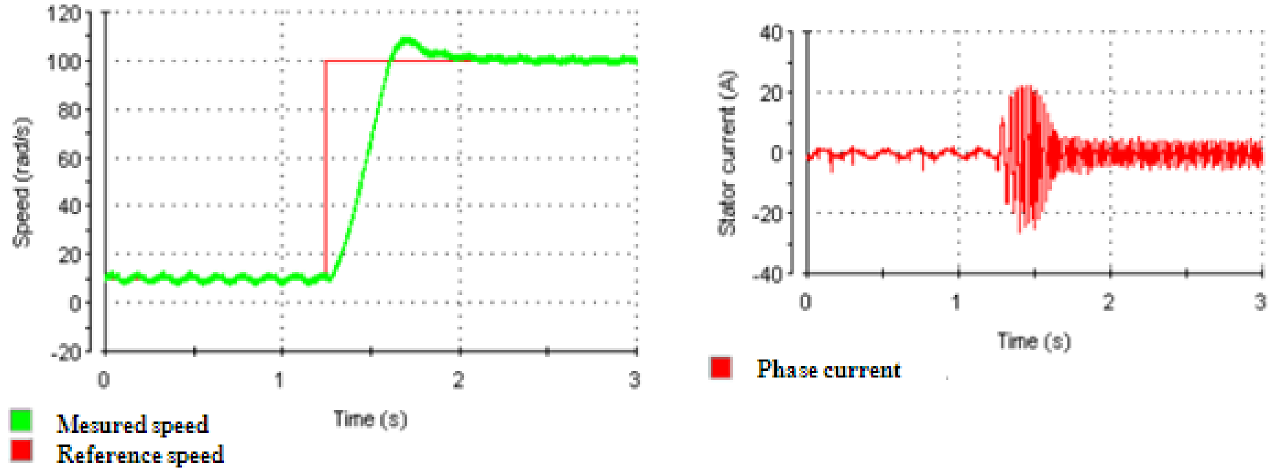

Fig. 8. Functioning in step reference speed (10 rd/s to 100 rd/s)

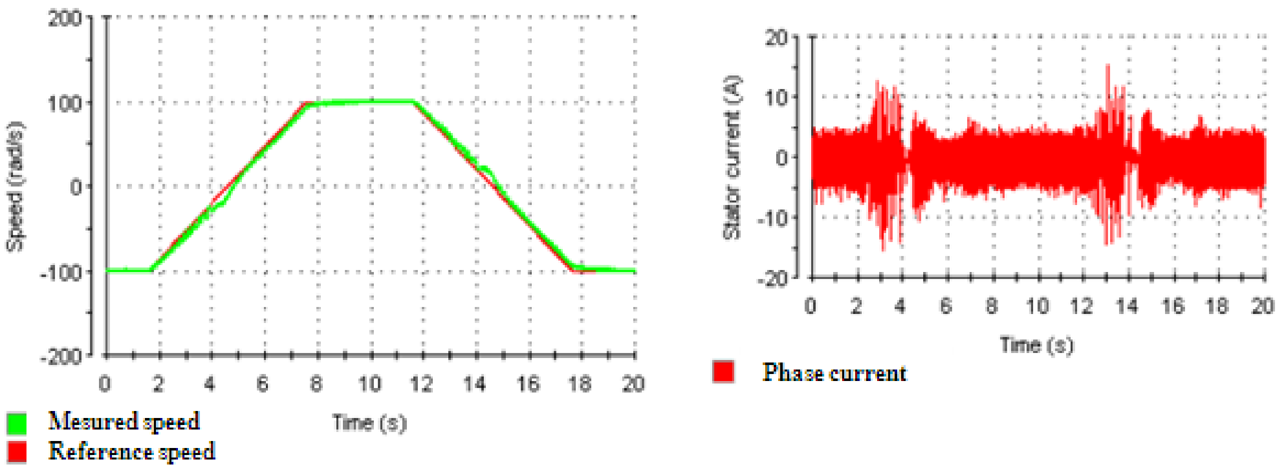

Fig. 9. Functioning in variation reference speed (-100 rd/s to 100 rd/s)

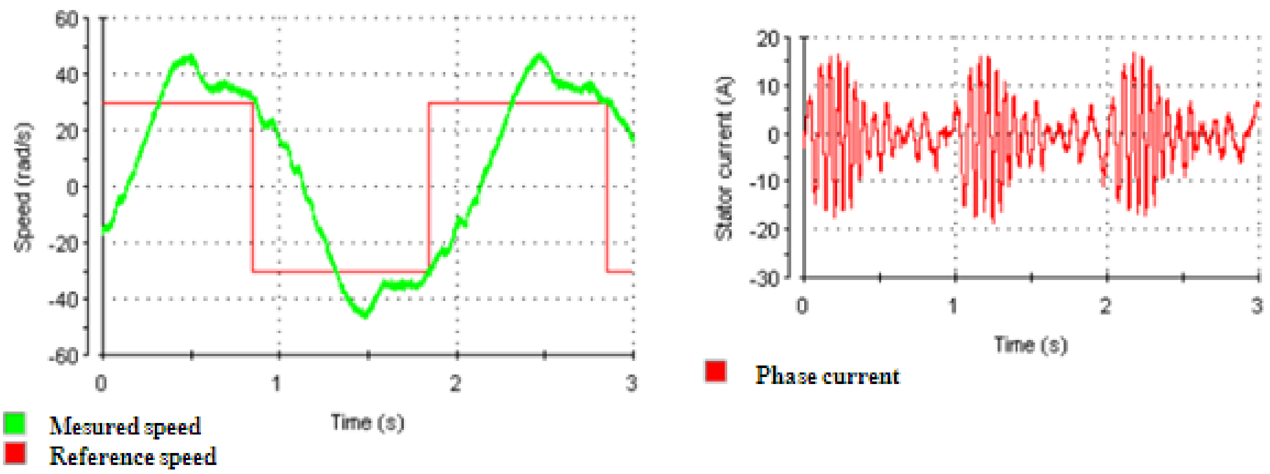

Fig. 10. Functioning at low speed (±30rd/s)

5.2 Experimental results for RFOC strategy:

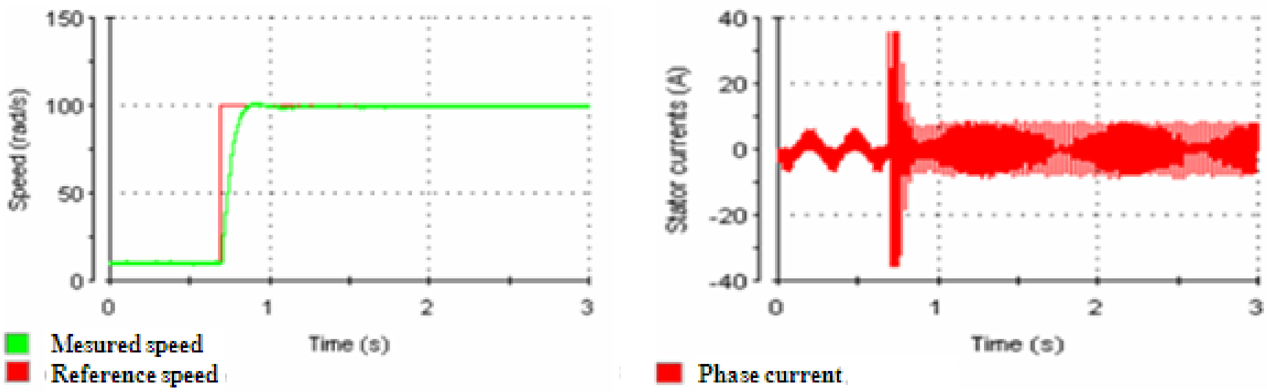

Fig. 11. Functioning in step reference speed (10 rd/s to 100 rd/s)

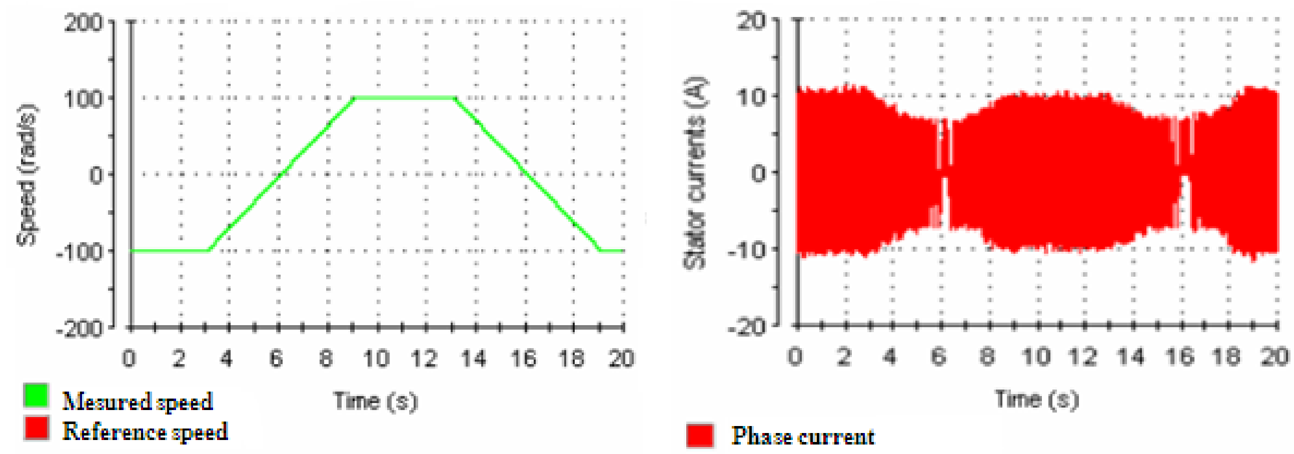

Fig. 12. Functioning in variation reference speed (-100 rd/s to 100 rd/s)

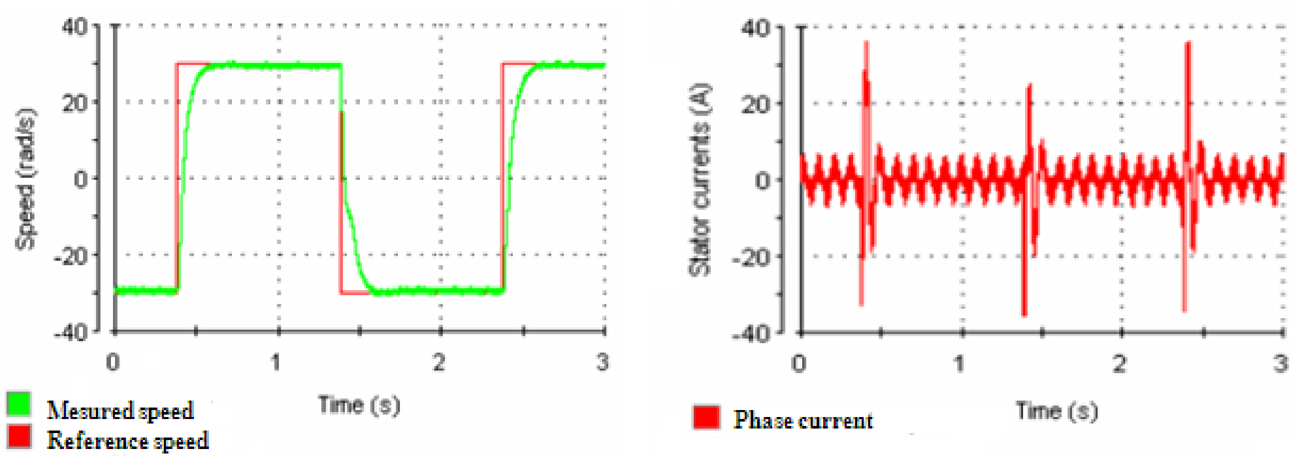

Fig. 13. Functioning at low speed (±30rd/s)

The results presented in the various figures show comparison experimental results between different controls. For the constant V/f principle, its practical application at low frequency is still challenging, due to the influence of the stator resistance and the necessary rotor slip to produce torque. But, control RFOC strategy, show good results in transient conditions and even in low speed. The stator phase current in the induction motor remains sinusoidal and takes appropriate value. Speed loop control using a fuzzy logic controller is good for the different cases considered.

6. Conclusion

With the introduction of solid-state inverters, the constant V/f control became popular, and the great majority of variable speed drives in operation today are of this type . However, since the introduction of vector control theory by Blaschke [5], almost all research has been concentrated in this area.

This paper presents experimental results of an efficient speed control based constant V/f principle and RFOC strategy for 3kw induction motor drives. The first strategy has poor control during the transient conditions and low speeds. This result is expected because the principle of V / f constant is based on the equations of induction machine in steady-state.

Anyway, the results were satisfactory and the proposed PI Fuzzy controller gives the system good performance and good dynamic behavior. The proposed controller schemes are implemented on the dSPACE DS1104 through personal computer utilizing a DSP processor TMS320F240 of Texas instruments.

Appendix:

Rated power	3 KW
Voltage	380V Y
Frequency	50 Hz
Pair pole	2
Rated speed	1400 rpm
Stator resistance	1.7 Ω
Rotor resistance	2.68 Ω
Inductance stator	229 mH
Inductance rotor	229 mH
Mutual inductance	217 mH
Moment of Inertia	0.046 kg.m^2

Table 2: Parameters motor induction

Photograph of the experimental setup

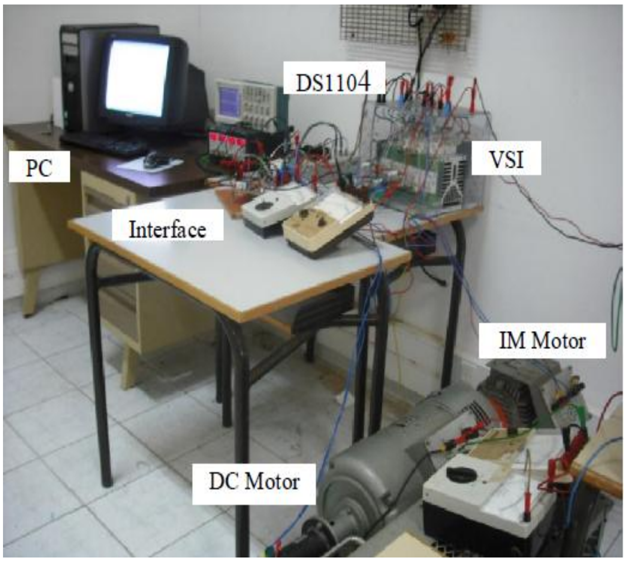

References:

[1] D.Casadei,F. Profumo, G.Serra and A. Tani, FOC and DTC: Tox viable schemes for induction motors Torque control, *IEEE Trans. Power Electronics*, vol. 17, n° 5, Sept 2002.

[2] C. Chakraborty and Y. Hori, Fast Efficiency Optimized Technique for the Indirect Vector Controlled Induction Motor Drives, *IEEE Trans. Ind. Appl*., Vol.39, pp.1070-1076, July/Aug., 2003.

[3] B.Nahid-Mobarakeh, F. Betin, D. Pinchon and G.A. Capolino, Sensorless field oriented control of induction machines using a reduced order linear disturbance observer, *Electromotion,* , Marrakesh, vol. 10, pp. 545–550, Oct. 2003.

[4] A. Abbou, H. Mahmoudi, Design of a New Sensorless Control of Induction Motor using Backstepping Approach, *International Review of Electrical Engineering*, vol.3, N.1, pp.166-173, Junuary-February 2008.

[5] F. Blaschke, The principle of field orientation as applied to the new transvektor closed-loop control system for rotating-field machines, *Siemens Rev.*, vol. 34, pp. 217–220, 1972.

[6] K. Koga, R. Ueda, and T. Sonoda, Constitution of V/f control for reducing the steady state speed error to zero in induction motor drive system, in *Conf. Rec. IEEE-IAS Annu. Meeting*, 1990, pp. 639–646.

[7] B. K. Bose, *Modern Power Electronics and AC Drives*, (Pearson Education, Inc. 2002).

[8] I. Takahashi, Direct Y.Ohmori, High-performance Torque Control of year Induction Motor, IEEE Transactions one Industry Applications, vol. 25, pp. 257-264, March/April 1989.

[9] J. Holtz, Sensorless Control of induction motor drives , *Proc.IEEE*, vol. 90, n°8, pp.1359-1394, 2002.

[10] Y. Sayouti, A. Abbou**,** M. Akherraz , H. Mahmoudi **,** Fuzzy speed control of induction motor with DTC-based Neural Network , Journal of Theoretical and Applied Information Technology, Vol.4, N°8,pp.747-752, 2008.

[11] Tsuji, M., Chen, S., Izumi, K., Yamada, A sensorless vector control system for induction motors using q-axis flux with stator resistance identification , *IEEE Tran. Ind. Electron*, Vol. 48 No.1, pp.476-83.2003.

[12] G. Bottiglieri, G. Scelba, G. Scarcella, A. Testa, A. Consoli, Sensorless Speed Estimation in Induction Motor Drives , *proc. of IEEE IEMDC*, 1-4 June 2003, Madison, pp. 624 - 630.

[13] N.Teske, G.M.Asher, M.Sumner and K.J. Brad ley, Suppression of Effects for the sensorless saturation saliency position control of induction motor drives under loaded condition, *IEEE Tran. On Indus. Electronics*, Vol. 47, No.5, pp. 1142-1149, 2000.

[14] D. Casadei and G. Serra, Implementation of direct torque control algorithm for induction motors based on discrete space vector modulation, *IEEE Trans. Power Electronics*, vol.15, N°4, July2002.

[15] M. Boussak, Implementation and experimental investigation of sensorless speed control of permanent magnet synchronous motor drive, *IEEE Transactions on Power Electronics*, vol. 20, n°6, pp. 1413–1422, Nov./Dec. 2005.

[16] G.MadhusudhanaRao, Dr.B.V.SankerRam, A Neural Network Based Speed Control for DC Motor, *International Journal of Recent Trends in Engineering*, Vol 2, No. 6, November 2009.

[17] Sung-Hoe Huh, Kyo-Beum Lee, Dong-Won Kim, Ick Choy, and Gwi-Tae Park, Sensorless Speed Control System Using a Neural Network, *International Journal of Control, Automation, and Systems*, vol. 3, no. 4, pp. 612-619, December 2005.

[18] Chao Yang and J. W. Finch, A Comparison of Induction Motor Speed Estimation using Conventional MRAS and AI Based MRAS with a Dynamic Reference Model, *Proceedings of the World Congress on Engineering*, Vol. I, 2008.

[19] L. Ben-Brahim, S. Tadakuma, A. Akdag, Speed control of induction motor without rotational transducers, IEEE Trans. Ind. Appl., vol.35, no.4, pp.844–850, Jul./Aug.1999.

[20] H.Kubota, K.Matsuse, and T.Nakano, DSP-based speed adaptive Flux observer of induction motor, IEEE Trans. Ind. Appl. , vol. 29, no.2, pp. 344–348, Mar./Apr.1993.

[21] H.Kubota, K.Matsuse, and Y.Hori, Behavior of sensorless induction motor drives in regenerating mode, in Proc.PCC'97, vol. 2, Nagaoka, Japan, pp.549–552.

[22] S.Kim, T.Park, J.Yoo, and G.Park, Speed-sensorless vector control of an induction motor using neural network speed estimation, IEEE Trans. Ind.Electron., vol. 48, no. 3, pp. 609–614, June. 2001.

[23] Y. Sayouti, A . Abbou, M. Akherraz, H. Mahmoudi, Real-time DSP implementation of DTC neural network-based for induction motor drive, PEMD 2010, vol. 3, pp. 1-5, April 2010.

[24] M. Cirrincione, M. Pucci, An MRAS-based sensorless high-performance induction motor drive with a predictive adaptive model, IEEE Trans. Industrial Electronics, Vol. 52 no. 2, pp. 532- 551, April 2005.

[25] C. Shauder, Adaptive Speed identification for Vector Control of Induction Motors without Rotational Transducers, IEEE Trans. Industry Applications, vol.. 28, no. 5, pp. 1054-1061, September/October 1992.

[26] D.W. Jin Y.A. Kwon. A novel mras based speed sensorless control of induction motor . IECON 99, Nov./Dec 1999, Vol. 2 pp. 933-938.

AUTHORS' INFORMATION

L2EP,

Electric Engineering Department,

The Mohammadia School's of engineers,

Mohamed V University Agdal

Morocco.

A. Abbou: Was born in AGADIR, Morocco, in September 19, 1973. He received the B.S. and Aggregation in electrical engineering from ENSET Rabat, Morocco in 1997 and 2000 respectively, and received the M.S. degree in industrial electronics and the Ph.D. degree in electrical engineering from Mohammadia School's of Engineers, Morocco, in 2009. Since 2010, he has been a Professor at the Mohammadia School's of engineers, Rabat, Morocco,

He has presented papers at national and international conferences on the Electrical machines, Power Electronics and Electrical drives.

His current area of interest is related to the innovative control strategies for AC Drives, especially Induction Motor Drives, RFOC, DTC, Backstepping and Sensorless Control. At present, we make Hardware experimental in RTW with DS1104 board from dSPACE piloted by the processor TMS320F240.

H. Mahmoudi: was born in Meknes, Morocco, on January 4, 1959. He received the B.S degree in electrical engineering from Mohammadia School's of engineers, Rabat, Morocco, in 1982, and the Ph.D. degree in power electronic from Montefiore Institute of electrical engineering, Luik, Belgium, in 1990.
He was an Assistant Professor of physics, at the

Faculty of sciences, Meknes, Morocco, from 1982 to 1990. Since 1992, he has been a Professor at the Mohammadia School's of engineers, Rabat, Morocco, and he was the Head of Electric Engineering Department during four years (1999, 2000, 2006 and 2007).
His research interests include static converters, electrical motor drives, active power filters and the compatibility electromagnetic.